

## Supplementary Information

### A. Field-effect enzymatic detection

Redox enzymes are immobilized on the sensing electrodes of biosensors as sensing elements. The active sites of redox enzymes are embedded in a three dimensional polypeptide network. The isolation of the active site by the polypeptide network causes low level of interfacial electron transfer between the enzyme and the electrode of a biosensor, creating a fundamental limit on the sensitivity of amperometric biosensors. In general, the detection limit of conventional biosensors is in the micro molar ( $10^{-6}$  M) analyte range.

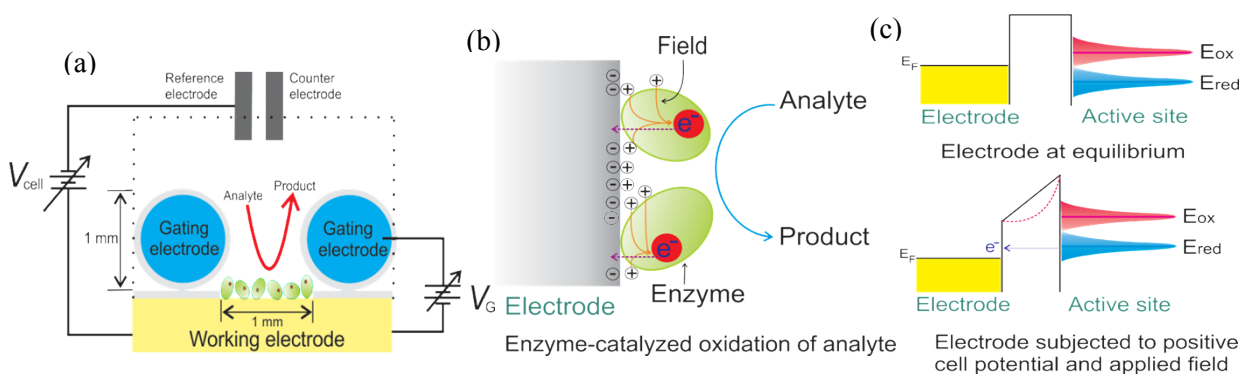


Figure A1 (a) Cross-sectional view of the field-effect bio-detection setup. Each elliptical structure represents an enzyme molecule. The enzyme's active center is indicated by the smaller circle within a molecule. The gating electrodes are represented by the circular structures, which consist of a copper wire (the blue circles) and a thin layer of insulator (the shaded shells).  $V_G$  is a voltage source used to produce an electric field between the sample solution and the working electrode. (b) Conceptual description of enzyme-electrode interface. The red dot is the active site of the enzyme. The double layer and induced charges are indicated. The induced charge set up the field within the enzyme. The enzyme catalyzes the oxidation of the analyte, resulting in electrons  $e^-$  transferred from the active site to the electrode. (c) The effect of the  $V_{cell}$  and that of the induced electric field is depicted using the interfacial electron energy profile.

Figure A1 (a) is a schematic description of the detection system. It consists of a conventional three-electrode electrochemical cell with a cell potential  $V_{cell}$  connected between the working electrode and the reference electrode. Under the normal operation condition, an electric double layer is present near the surface of the working (sensing) electrode. The cell is modified with additional gating electrodes for applying a gating voltage  $V_G$  between the gating electrode and the

working electrode, upon which a redox enzyme is immobilized.  $V_G$  modified the interfacial charge distribution. When  $V_G$  is positive, additional negative charges are induced within the working electrode and additional positive ions in solution are induced at the solution-enzyme-electrode interface. Figure A1 (b) depicts the net interfacial charge distribution. Some positive ions are able to set up electric fields with the presence of the transferring electrons residing at the enzyme's active sites (the red circles) as indicated in Figure A1 (b). The fields lower the potential energy experienced by the transferring electrons in the polypeptide region between the active sites and the electrode.<sup>23, 24</sup>

The signal current of a biosensor using immobilized redox enzyme as the sensing element is the result of quantum mechanical tunneling of electrons from the active site of the enzyme through the polypeptide tunnel barrier to the electrode. The energy profile of tunnel barrier can be modified by an electric field so that the tunneling rate is enhanced. As explained above (see Figure A1 (b)), the induced fields lowers the height of the tunnel barrier (the potential energy experienced by the transferring electrons) and therefore increases the electron tunnel rate and hence the current. The result of this process is an amplified signal current.

Figure A1 (c) shows a conceptual energy-band profile of the enzyme-electrode interface. At equilibrium, no electron transfer occurs between the active site and the electrode, since the most probable energy of the occupied quantum state of the active site,  $E_{red}$ , is below the Fermi energy  $E_F$  of the electrode. When the cell potential  $V_{cell}$  is raised, oxidation of the enzyme occurs as electrons are energetically allowed to be transferred from the  $E_{red}$  to the electrode. The electrode-active site system can be considered as a acceptor-donor pair, and the electron transfer rate

constant  $k_{et}$  depends critically on the distance  $d$  between the electrode and the active site as  $k_{et} \propto \exp(-\beta d)$ .<sup>25</sup> The exponential dependence of  $k_{et}$  on  $d$  effectively diminishes electron transfer. However, the rate constant also depends on the value of the attenuation coefficient,  $\beta$ , which is proportional to the square root of the tunnel barrier height ( $\beta \propto (\Phi_B)^{1/2}$ ). When  $V_G$  is turned on, the induced electric field distorts the top of the tunnel barrier (see the red dashed curve), reducing the effective height of the barrier<sup>24, 26</sup> and, therefore, resulting in a smaller value of  $\beta$  and therefore a larger value of  $k_{et}$ . Thus, electron conduction in the nanoscale region between the active site and the electrode is enhanced, resulting in increased analyte oxidation current (amplified signal) and therefore lowered detection limit.

In this work, the enzyme in Figure A1 (a) is replaced by the antibody-antigen-antibody (Ab-Ag-Ab) immune complex as shown in Figure A2, where the antigen is *E. coli* and the secondary antibody is labeled with HRP. The induced electric field penetrates the complex and reduces its electric resistance.

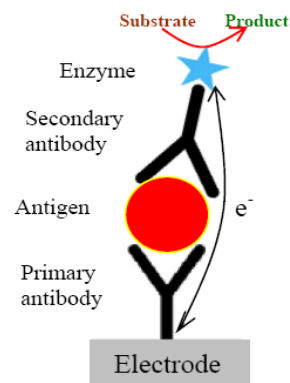


Figure A2 The sandwich Ab-Ag-Ab immune complex of amperometric immuno-

1. E. Csoregi, S. Gaspar, M. Niculescu, B. Mattiasson and W. Schuhmann, ed. M. D. Cuyper and J. W. M. Bulte, Kluwer Academic Publishers, Dordrecht, Boston, London, 2001, vol. 7, p. 105.
2. J. D. Jackson, *Classical Electrodynamics*, John Wiley & Sons, Inc., Danvers, 1998.
3. R. A. Marcus and N. Sutin, *Biochim. Biophys. Acta*, 1985, **811**, 265.
4. S. J. Tans, A. R. M. Verschueren and C. S. J. Dekker, *Nature*, 1998, **393**, 49.

## B. Control and related measurements

Figure B1 shows a set of CVs obtained under different conditions with a PG electrode modified with PANI and glutaraldehyde as described in the text. The modified electrode was first immobilized with the primary Ab and subsequently with the labeled secondary Ab(HRP). Then, the electrode was rinsed with PBS to remove unstable structures from the electrode. CV1 was obtained with this electrode in PBS containing 10 mM H<sub>2</sub>O<sub>2</sub>. CV2 was obtained with the same electrode in H<sub>2</sub>O<sub>2</sub> when a V<sub>G</sub> of 0.6 V was applied. The two CVs appear to be featureless and have similar magnitudes. Similar results as shown in Figure A2 were obtained with the modified electrode, which was first immobilized with *E. coli* O157:H7, subsequently immobilized with secondary Ab(HRP) to form the *E. coli*-Ab(HRP) structure and finally rinsed with PBS. The absence of redox peaks in Figure B1 and Figure B2 indicates that the HRP-labeled antibody and hence HRP is not immobilized on the electrode under the conditions specified for the figures so that no signals will be detected. HRP can be immobilized on the electrode via the formation of the Ab-*E.coli*-Ab(HRP) complex so that the detection signal is produced. Additional experiments were performed to clarify the experimental conditions. In order to eliminate the possibility that H<sub>2</sub>O<sub>2</sub> can be reduced by the electrode in the absence of HRP, CVs with and without H<sub>2</sub>O<sub>2</sub> were obtained with electrodes whose surface were modified with PANI and glutaraldehyde, blocked with BSA and immobilized with the components of the immune reaction except for the HRP-labeled antibody. Figure B3 shows two sets of CVs obtained for this purpose. The upper set was obtained with a modified and blocked electrode, which was immobilized with the primary antibody. The lower set was obtained with a modified and blocked electrode immobilized with *E. coli*. CV1 and CV3 were obtained in PBS while CV2 and CV4 in PBS with H<sub>2</sub>O<sub>2</sub>. The CVs show that the presence of H<sub>2</sub>O<sub>2</sub> produced insignificant effects. Also, experiments using graphite

electrodes without PANI but with glutaraldehyde and the sandwich immune complex resulted in no observable signal.

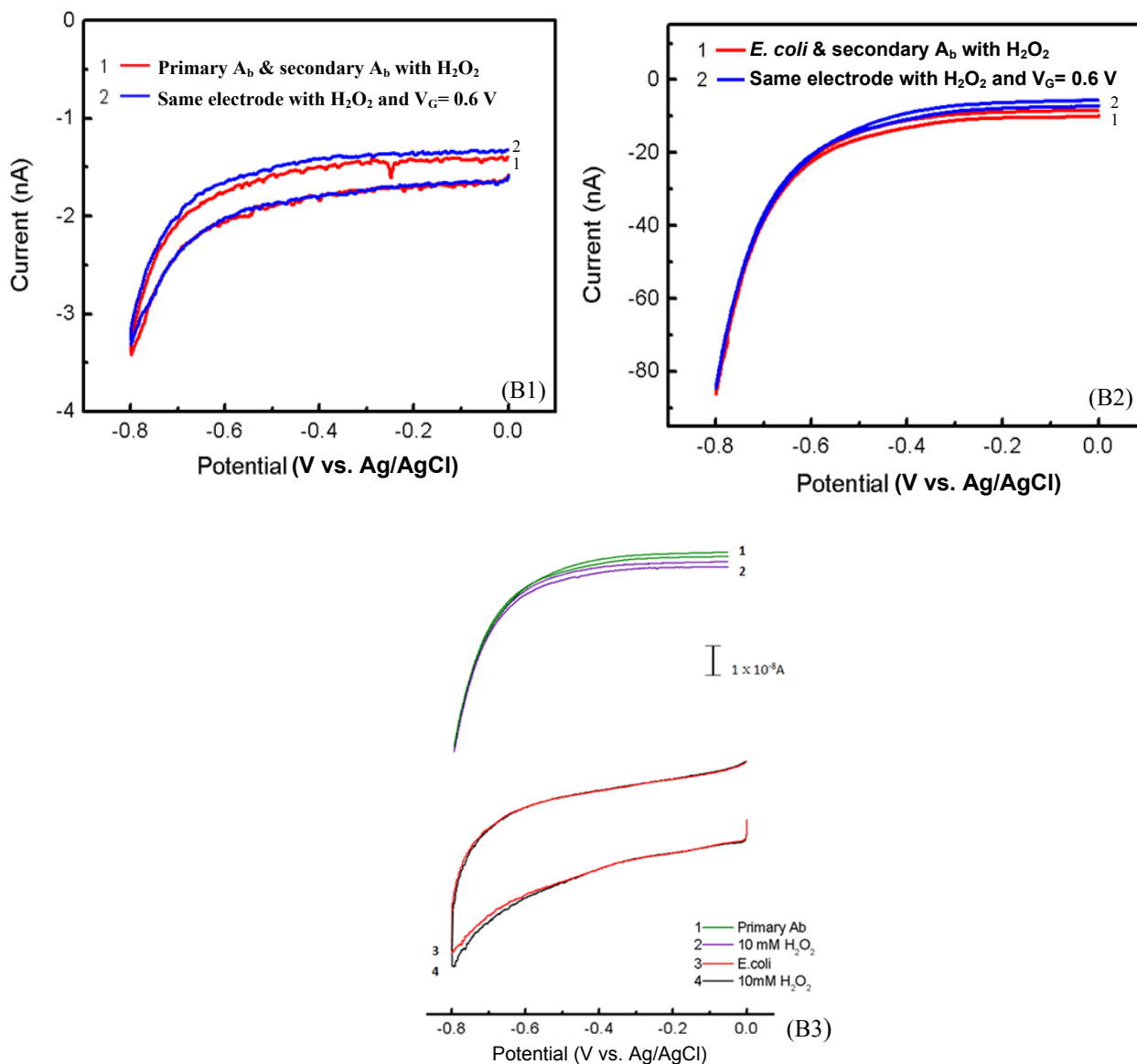


Figure B1 Control experiments performed with immobilized primary antibody and HRP-labeled secondary antibody under different conditions as stated in the figure.

Figure B2 Experiments performed with immobilized *E. coli* O157:H7 and HRP-labeled secondary antibody under different conditions as stated in the figure.

Figure B3 Two sets of CVs used to show that H<sub>2</sub>O<sub>2</sub> is not reduced by the modified electrode.